



CHORUS

This is the accepted manuscript made available via CHORUS. The article has been published as:

New Patterns of Activity in a Pair of Interacting Excitatory-Inhibitory Neural Fields

S. E. Folias and G. B. Ermentrout

Phys. Rev. Lett. **107**, 228103 — Published 21 November 2011

DOI: [10.1103/PhysRevLett.107.228103](https://doi.org/10.1103/PhysRevLett.107.228103)

New Patterns of Activity in a Pair of Interacting Excitatory-Inhibitory Neural Fields

S. E. Folias¹ and G. B. Ermentrout¹

¹*Department of Mathematics, University of Pittsburgh, Pittsburgh, PA*

In this Letter, we study stationary bump solutions in a pair of interacting excitatory-inhibitory (E-I) neural fields in one dimension. We demonstrate the existence of localized bump solutions of persistent activity that can be maintained by the pair of interacting layers when a stationary bump is not supported by either layer in isolation—a scenario which may be relevant as a mechanism for the persistent activity associated with working memory in the prefrontal cortex and may explain why bumps are not seen in *in vitro* slice preparations. Furthermore, we describe a new type of stationary bump solution arising from a pitchfork bifurcation which produces a stationary bump in each layer with a spatial offset that increases with the bifurcation parameter.

PACS numbers: 87.19.lp, 87.19.lv, 87.10.-e, 05.45.-a

Delayed-response task experiments in awake monkeys have identified persistent activity in the prefrontal cortex as a neural correlate of spatial working memory [1–3]. Different neurons in the prefrontal cortex are capable of encoding and storing different spatial locations to form a mnemonic map of the visual field [2]. Stationary bumps arising in excitatory-inhibitory neural fields or Wilson-Cowan models [4–6] have been used to model persistent activity in the prefrontal cortex [6–9]. Though such studies demonstrate that single-layer neural field models are capable of supporting localized persistent activity, *in vitro* slice preparations of cortical tissue tend to exhibit more dynamic and transitory behavior and have not been shown to support bump-like persistent activity. While this may be the consequence of important connections being disrupted or destroyed in the slice preparation, it is plausible that the persistent activity is alternatively maintained by the interaction between two (or more) reciprocally connected layers or brain regions. Indeed, other brain regions exhibit persistent activity concurrently during the delayed-response tasks, e.g., posterior parietal cortex and thalamus [10, 11], and both form reciprocal connections with prefrontal cortex.

Hence, one significant result of this Letter is to demonstrate that a stable stationary bump of activity can be supported by a *pair* of interacting neural field layers when each layer in isolation does *not* support a stable bump. We briefly introduce a model for *an interacting pair of E-I neural field layers* as illustrated in Fig. 1:

E-I Layer I

$$\begin{aligned}\tau_e \partial_t u_e + u_e &= w_{ee}^{loc} * f_e(u_e) - w_{ei}^{loc} * f_i(u_i) + w_{ee}^{lay} * f_e(v_e), \\ \tau_i \partial_t u_i + u_i &= w_{ie}^{loc} * f_e(u_e) - w_{ii}^{loc} * f_i(u_i) + w_{ie}^{lay} * f_e(v_e),\end{aligned}$$

E-I Layer II

$$\begin{aligned}\tau_e \partial_t v_e + v_e &= w_{ee}^{loc} * f_e(v_e) - w_{ei}^{loc} * f_i(v_i) + w_{ee}^{lay} * f_e(u_e), \\ \tau_i \partial_t v_i + v_i &= w_{ie}^{loc} * f_e(v_e) - w_{ii}^{loc} * f_i(v_i) + w_{ie}^{lay} * f_e(u_e),\end{aligned}$$

where $w * f(u) = \int_{\mathbb{R}} w(x-y) f(u(y,t)) dy$.

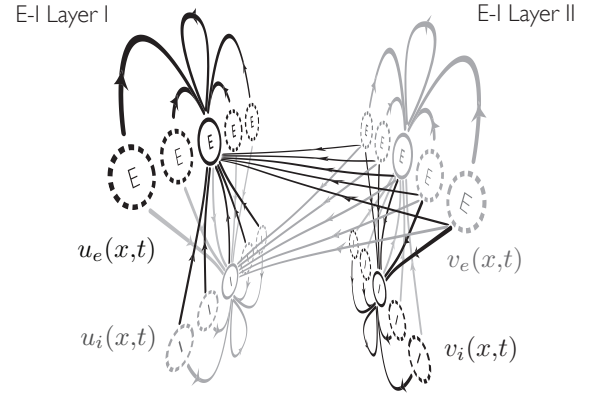


FIG. 1: A network composed of an interacting pair of excitatory-inhibitory (E-I) neural field layers. The E-I subnetworks interact through *reciprocally symmetric* interlayer synaptic interactions $w_{ee}^{lay}, w_{ie}^{lay}$ mediated by the excitatory populations u_e, v_e within each subnetwork. For simplicity, only connections from Layer II to Layer I are shown.

Neural fields are pattern-forming systems composed of nonlocal integrodifferential equations that share similar behavior with reaction-diffusion equations [4–6]. We assume the distance-dependent synaptic weight functions w_{uv}^l for $u, v \in \{e, i\}$ and $l \in \{loc, lay\}$ are even-symmetric and homogeneous (i.e., translationally invariant) in each one-dimensional layer. The layers have identical *local* connections w_{uv}^{loc} and reciprocally symmetric *interlayer* connections w_{ue}^{lay} that project only from the excitatory populations. The interlayer synaptic coupling determines a relationship between the coordinate systems for each layer; we define a *universal coordinate system* for both layers (*i*) using the local connections to determine the length scale in each layer and (*ii*) using the center point of the even-symmetric interlayer weight functions to identify the origin in Layer II based on the connections to the origin in Layer I and vice-versa.

We define the term *synaptic bump* (*syn + topos* mean-

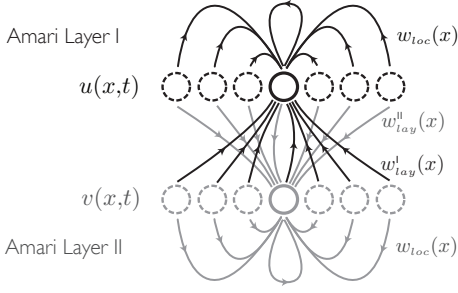


FIG. 2: A pair of interacting Amari neural field layers in which the even-symmetric interlayer synaptic coupling (w_{lay}^I, w_{lay}^{II}) determines a universal coordinate system for the two layers.

ing *together in place*) to refer to the case of a stationary bump in each E-I subnetwork if the two bumps share the same *center* in the universal coordinate system. The syntopic bump can undergo a bifurcation to new type of stationary bump that we call an *allotopic bump*, which is composed of a stationary bump in each layer with centers that are spatially offset. As the analysis of the full model is cumbersome, the results will instead in a forthcoming paper [12] with some of the results discussed briefly below. In this Letter, we concentrate on an important reduction wherein each E-I layer in Fig. 1 is simplified to an Amari neural field ([5, 9]) as illustrated in Fig. 2. The two models exhibit related structure and behavior, including syntopic and allotopic bumps (see Fig. 3).

The model for *an interacting pair of identical Amari neural field layers* is given by

$$\tau \partial_t u = -u + w_{loc} * H(u - \theta) + w_{lay}^I * H(v - \theta), \quad (1)$$

$$\tau \partial_t v = -v + w_{loc} * H(v - \theta) + w_{lay}^{II} * H(u - \theta). \quad (2)$$

H is the Heaviside function with a firing threshold θ . The local connections (w_{loc}) within each layer are given by a Mexican hat synaptic weight function and the *interlayer* connections (w_{lay}) are taken to be reciprocally symmetric so that $w_{lay}^{II} \equiv w_{lay}^I \equiv w_{lay}$. Without loss of generality we take $\tau = 1$, and for calculations, we use general synaptic weight functions of the form

$$w_l(x) = \frac{1}{2} \frac{A_l^e}{\sigma_l^e} e^{-\frac{|x|}{\sigma_l^e}} - \frac{1}{2} \frac{A_l^i}{\sigma_l^i} e^{-\frac{|x|}{\sigma_l^i}}, \quad l \in \{loc, lay\}.$$

The reduction from an E-I layer to an Amari layer can be validated by assuming (i) the inhibitory population is in quasisteady state ($\tau_i = 0$), (ii) no inhibitory-to-inhibitory coupling ($w_{ii}^{loc} = 0$), (iii) a linear firing rate function for the inhibitory population ($f_i(u_i) = u_i$) and a Heaviside firing rate function for the excitatory population ($f_e(u_e) = H(u_e - \theta)$) [9]. Under these same assumptions, the pair of interacting E-I layers analogously reduces to (1)-(2) with $w_{loc} = w_{ee}^{loc} - w_{ei}^{loc} * w_{ie}^{loc}$ and $w_{lay} = w_{ey}^{lay} - w_{ei}^{loc} * w_{ie}^{lay}$ [12].

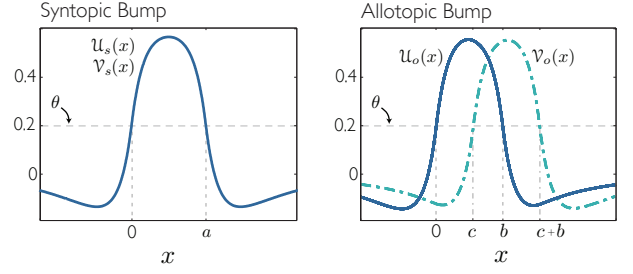


FIG. 3: LEFT: Stationary syntopic bump profile $\mathcal{U}_s = \mathcal{V}_s$ in the pair of symmetrically interacting ($w_{lay}^I \equiv w_{lay}^{II} \equiv w_{lay}$) Amari layers where \mathcal{U}_s is the stationary bump in Layer I and \mathcal{V}_s is the stationary bump in Layer II. RIGHT: Stationary allotopic bump with \mathcal{U}_o denoting the stationary bump in Layer I and \mathcal{V}_o denoting the stationary bump in Layer II. Both bumps have width b and are separated by a distance c .

We analyze the existence and linear stability of a stationary *syntopic bump* which is composed of bumps $u(x,t) = \mathcal{U}_s(x)$ in Layer I and $v(x,t) = \mathcal{V}_s(x)$ in Layer II, with $\mathcal{V}_s(x) \equiv \mathcal{U}_s(x)$. This represents a stationary bump in each layer with identical spatial profiles that are localized about the same *center* in the universal coordinate system. The spatial profile $\mathcal{U}_s(x)$ of the syntopic bump must satisfy threshold conditions $\mathcal{U}_s(0) = \mathcal{U}_s(a) = \theta$, where a is the *syntopic bump width*, and we require the bump in each layer to be superthreshold ($\mathcal{U}_s(x) > \theta$) over the spatial region $(0, a)$ and be subthreshold ($\mathcal{U}_s(x) < \theta$) otherwise with $\mathcal{U}_s(x) \rightarrow 0$ as $x \rightarrow \pm\infty$. The stationary syntopic bump $(u, v)^T = (\mathcal{U}_s, \mathcal{U}_s)^T$ can be expressed as

$$\mathcal{U}_s(x) = [W_{loc}(x) - W_{loc}(x-a)] + [W_{lay}(x) - W_{lay}(x-a)]$$

where $W_l(x) \equiv \int_0^x w_l(y) dy$ for $l \in \{loc, lay\}$. The threshold condition $\mathcal{U}_s(0) = \mathcal{U}_s(a) = \theta$ yields a compatibility condition that determines the syntopic bump width a

$$\theta = W_{loc}(a) + W_{lay}(a) \quad (3)$$

guaranteeing the existence of a stationary syntopic bump, provided the assumptions on \mathcal{U}_s are satisfied.

We highlight an important way in which a syntopic bump can emerge in a pair of identical Amari layers. If the local connections w_{loc} are of Mexican hat type (e.g., $\sigma_{loc}^i > \sigma_{loc}^e$ and $A_{loc}^i < A_{loc}^e$) but, alone, do *not* support a stationary bump (i.e., $W_{loc}(a) < \theta$ for all $a \in (0, \infty)$), the inclusion of excitatory ($w_{lay} > 0$) interlayer connections can generate a stable stationary syntopic bump through a saddle-node bifurcation as illustrated in Fig. 4. There is bistability between the syntopic bump and the spatially homogeneous rest state. In numerical simulations, when the interlayer connections are removed, the activity rapidly approaches the rest state. We also mention that it is additionally possible to generate stable syntopic bumps with excitatory interlayer connections even when

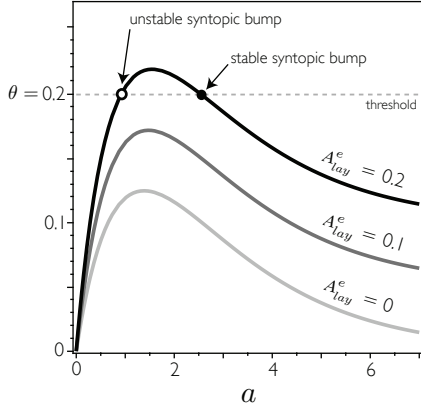


FIG. 4: Plots of $[W_{loc}(a) + W_{lay}(a)]$ in (3) for various values of A_{lay}^e with $A_{lay}^i = 0$. In the absence of interlayer connections ($A_{lay}^e = 0$), the local connections within each layer do not support a stationary bump (since $W_{loc}(a) < \theta$ for $a > 0$). Increasing the excitatory interlayer coupling strength $A_{lay}^e > 0$ leads to a saddle-node bifurcation of syntopic bumps and, for the following parameters, the larger syntopic bump that emerges is stable (from linear stability analysis). Fixed parameters are $A_{loc}^e = A_{loc}^i = \sigma_{loc}^e = 1, \sigma_{loc}^i = 2, \sigma_{lay}^e = 0.5, \theta = 0.2$

the extent of the local excitatory connections exceed the local inhibitory connections (i.e., not a Mexican hat) [12].

To study the linear stability of the syntopic bump, we consider the evolution of arbitrary, small perturbations of the solution $(\mathcal{U}_s, \mathcal{V}_s)^T$, where $\mathcal{V}_s(x) = \mathcal{U}_s(x)$, by setting

$$u(x, t) = \mathcal{U}_s(x) + \varphi(x)e^{\lambda t}, \quad v(x) = \mathcal{V}_s(x) + \psi(x)e^{\lambda t}$$

in the linearization about the syntopic bump which leads to the spectral problem

$$\begin{aligned} \lambda \varphi &= -\varphi + \mathcal{N}_{loc} \varphi + \mathcal{N}_{lay} \psi \\ \lambda \psi &= -\psi + \mathcal{N}_{loc} \psi + \mathcal{N}_{lay} \varphi \end{aligned} \quad (4)$$

where \mathcal{N}_{loc} and \mathcal{N}_{lay} are given for $l \in \{loc, lay\}$ by

$$\begin{aligned} \mathcal{N}_l \phi(x) &= \int_{\mathbb{R}} w_l(x-y) \delta(\mathcal{U}_s(y) - \theta) \phi(y) dy \\ &= \frac{w_l(x)}{|\mathcal{U}'_s(0)|} \phi(0) + \frac{w_l(x-a)}{|\mathcal{U}'_s(a)|} \phi(a) \end{aligned}$$

with $\mathcal{U}'_s(0) = -\mathcal{U}'_s(a) > 0$. The essential spectrum does not cause instability; the point spectrum is found by setting $x = 0$ and $x = a$ in (4) and solving $(M - I)\mathbf{v} = \lambda \mathbf{v}$

$$M = \begin{bmatrix} \hat{w}_{loc}(0) & \hat{w}_{loc}(a) & \hat{w}_{lay}(0) & \hat{w}_{lay}(a) \\ \hat{w}_{loc}(a) & \hat{w}_{loc}(0) & \hat{w}_{lay}(a) & \hat{w}_{lay}(0) \\ \hat{w}_{lay}(0) & \hat{w}_{lay}(a) & \hat{w}_{loc}(0) & \hat{w}_{loc}(a) \\ \hat{w}_{lay}(a) & \hat{w}_{lay}(0) & \hat{w}_{loc}(a) & \hat{w}_{loc}(0) \end{bmatrix}, \quad \mathbf{v} = \begin{pmatrix} \varphi(0) \\ \varphi(a) \\ \psi(0) \\ \psi(a) \end{pmatrix}.$$

where $\hat{w}_l(x) = w_l(x)/|\mathcal{U}'_s(0)|$, for $l \in \{loc, lay\}$. This matrix equation determines the eigenvalues λ and the associated eigenfunctions $(\varphi(x), \psi(x))^T$ by using \mathbf{v} in (4).

Using a similarity transformation $Q^{-1}(M - I)Q = \Lambda$, $(M - I)$ is similar to the block diagonal matrix Λ

$$\Lambda = \begin{bmatrix} \Lambda_+ - I_2 & 0 \\ 0 & \Lambda_- - I_2 \end{bmatrix}$$

where I_2 is the 2×2 identity matrix and

$$\Lambda_{\pm} = \begin{bmatrix} \hat{w}_{loc}(0) \pm \hat{w}_{loc}(a) & \hat{w}_{lay}(0) \pm \hat{w}_{lay}(a) \\ \hat{w}_{lay}(0) \pm \hat{w}_{lay}(a) & \hat{w}_{loc}(0) \pm \hat{w}_{loc}(a) \end{bmatrix}.$$

Setting $\gamma = |\mathcal{U}'_s(0)|$, the resulting four eigenvalues are

$$\begin{aligned} \lambda_+^+(a) &= \frac{2}{\gamma} (w_{loc}(a) + w_{lay}(a)), \\ \lambda_+^-(a) &= \frac{2}{\gamma} (w_{loc}(a) - w_{lay}(0)), \\ \lambda_-^-(a) &= -\frac{2}{\gamma} (w_{lay}(0) - w_{lay}(a)). \end{aligned}$$

and the zero eigenvalue $\lambda_+^-(a) = 0$ which reflects the translation invariance of the syntopic bump.

Interestingly, a special pitchfork bifurcation occurs when a syntopic bump loses stability as eigenvalue $\lambda_-^-(a)$ increases through 0, i.e., if $w_{lay}(0) = w_{lay}(a)$. This can occur when $w_{lay}(x)$ transitions from having a single peak at $x = 0$ to having an even-symmetric double peak with a local minimum at $x = 0$. The bifurcating solution reflects the geometry of the associated spatial eigenmode which corresponds to a lateral perturbation to one side of the stationary bump in one layer and to the opposite side of the stationary bump in the other layer [12]. Indeed, in neural field equations, the bifurcating solution commonly reflects a structure that is geometrically similar to the destabilizing eigenmode [13–15].

We refer to the bifurcating solution $(u, v)^T = (\mathcal{U}_o, \mathcal{V}_o)^T$ as a stationary *allotopic bump* (*allo + topos* meaning *other + place*) as it is composed of a stationary bump \mathcal{U}_o in Layer I and \mathcal{V}_o in Layer II which are separated by a distance c that depends on the bifurcation parameter (see Fig. 3 and Fig. 5). Due to symmetry conditions, \mathcal{V}_o is a reflection and a translation of \mathcal{U}_o expressed as

$$\mathcal{V}_o(x) = \mathcal{U}_o(-(x - c - b)).$$

b denotes the width of the spatial region where each bump is above threshold (i.e., $\mathcal{U}_o(x) > \theta$ for $x \in (0, b)$ and $\mathcal{V}_o(x) > \theta$ for $x \in (c, b + c)$ or with \mathcal{U}_o and \mathcal{V}_o switched). Accordingly, the threshold conditions that determine the existence of an allotopic bump are

$$\begin{aligned} \theta &= W_{loc}(b) - W_{lay}(c) + W_{lay}(c + b), \\ \theta &= W_{loc}(b) + W_{lay}(c) - W_{lay}(c - b). \end{aligned} \quad (5)$$

In Fig. 5, we solve (3) and (5) for the existence of a pair of stationary syntopic bumps, each undergoing a pitchfork bifurcation that gives rise to an allotopic bump. Linear stability analysis of the allotopic bump indicates the

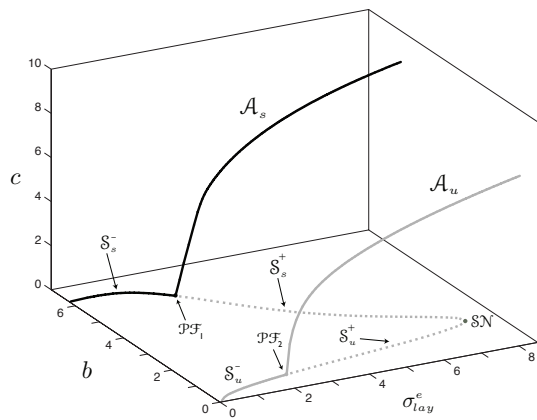


FIG. 5: Bifurcation diagram illustrating existence and stability of *syntopic* and *allotropic* bumps in a pair of interacting Amari layers (1)-(2) using (3) and (5). b denotes the bump width, c the distance between bumps, and σ_{lay}^e the bifurcation parameter. Syntopic bumps (i.e., $(b, c) = (a, 0)$) are stable along curve S_s^- and undergo a pitchfork bifurcation at \mathcal{PF}_1 , due to eigenvalue λ_-^- , giving rise to curve A_s of stable allotropic bumps and curve S_s^+ of unstable syntopic bumps. A_s represents two symmetrically related solutions in the pitchfork bifurcation. Unstable syntopic bumps along S_u^- also undergo a pitchfork bifurcation, and the two syntopic bumps annihilate in a saddle-node bifurcation at \mathcal{SN} . $A_{loc}^i = \sigma_{loc}^e = A_{loc}^i = 1, \sigma_{loc}^i = 5, A_{lay}^e = 0.5, A_{lay}^i = 0.4, \sigma_{lay}^e = 2, \theta = 0.2$.

bifurcations are supercritical in agreement with the geometry of the direction of bifurcation in Fig. 5.

We studied the existence of stationary *periodic* bumps with period L and analyzed their linear stability with respect to the class of L -periodic perturbations. Interestingly, a third type of spatially periodic, stationary solution can exist in which the periodic bump in one layer is shifted by half of a period ($L/2$) with respect to the periodic bump in the other layer, and we refer to it as the *antisyntopic periodic bump* since it is the spatial analogue of the antisynchronous solution in coupled-oscillator theory. The bifurcation structure is similar to that in Fig. 5, however, the difference is that the curve of allotropic periodic bumps terminates at a pitchfork bifurcation with the curve of antisyntopic periodic bumps, thereby stabilizing the remaining branch of antisyntopic bumps [12].

We additionally investigated the existence and linear stability of stationary syntopic bumps for reciprocally *asymmetric* interlayer synaptic coupling ($w_{lay}^i \neq w_{lay}^u$) which causes the bump in each layer generically to have different widths (but the same centers). Interestingly, while asymmetric interlayer coupling supports *stationary* syntopic bumps, loss of stability of the syntopic bump through the equivalent of eigenvalue λ_-^- in this case is found to give rise to a *travelling* allotropic bump in numerical simulations. From speed 0, the traveling wave speed increases with the disparity induced by the asymmetry in the interlayer connections [12].

In the interacting pair of E-I neural fields, we have investigated the existence and stability of solitary and periodic syntopic bumps in the case of excitatory *interlayer* connections. Two important results are that it is possible (i) to generate a stable stationary syntopic bump even if each E-I layer does not support a stationary bump and (ii) to stabilize a syntopic bump even if the spatial extent of the excitatory local connections within each layer exceed that of the inhibitory local connections. When a supercritical Hopf bifurcation occurs with respect to the pair of eigenvalues analogous to λ_+^+ , destabilization of the syntopic bump leads to time-periodic *breathers* simultaneously in each E-I network. Note, in [7, 9], it was shown that in the single E-I layer, a stable stationary bump can destabilize in a Hopf bifurcation if the dynamics of the inhibitory population are sufficiently slow ($\tau_i/\tau_e > \tau_{crit}$). In the dual E-I layers, for the parameter region we explored, τ_{crit} was found to vary from 1 to 40. It is also possible to generate a stationary *allotropic bump* by destabilizing the syntopic bump with respect to the equivalent of eigenvalue λ_-^- , and the spatial offset similarly varies with the bifurcation parameter. Syntopic bumps with different widths, traveling waves, and more complex spatiotemporal phenomena are also found [12].

Finally, as the cerebral cortex is a layered structure, an important extension is to consider two-dimensional spatial domains [14, 15] to study synaptic interactions between two interconnected layers of neural tissue which can be reasonably approximated as two-dimensional.

This work was supported by NSF grants EMSW21-RTG 0739261 and DMS-0817131.

-
- [1] P. S. Goldman-Rakic, *Neuron* **14**, 477-485 (1995).
 - [2] S. Funahashi, C. J. Bruce and P. S. Goldman-Rakic, *J. Neurophysiol.* **61**, 331-349 (1989).
 - [3] J. M. Fuster and G. E. Alexander, *Science* **173**, 652-654 (1971).
 - [4] H. R. Wilson and J. D. Cowan, *Kybernetik* **13**, 55 (1973).
 - [5] S. Amari, *Biol. Cybern.* **27**, 77-87 (1977).
 - [6] S. Coombes, *Biol. Cybern.* **93**, 91-108 (2005).
 - [7] P. Blomquist, J. Wyller and G.T. Einvoll, *Physica D* **206**, 180-212 (2005).
 - [8] C. Laing W. C. Troy B. Gutkin and G. B. Ermentrout, *SIAM J. Appl. Math.* **63**, 62-97 (2002).
 - [9] D. Pinto and G. B. Ermentrout, *SIAM J. Appl. Math.* **62**, 226-243 (2001).
 - [10] C. Constantinidis and M. A. Steinmetz, *J. Neurophysiol.* **76**, 1352-1355 (1996).
 - [11] J. M. Fuster and G. E. Alexander, *Brain Res.* **61**, 79-91 (1973).
 - [12] S. E. Folias and G. B. Ermentrout, *in preparation*, (2011).
 - [13] S. E. Folias, *SIAM J. Appl. Dyn. Syst.* **10**, 744-787 (2011).
 - [14] S. E. Folias and P. C. Bressloff, *Phys. Rev. Lett.* **95**, 208107 (2005).
 - [15] C. Laing and W. C. Troy, *SIAM J. Appl. Dyn. Syst.* **2**, 487-516 (2003).